ISTITUTO NAZIONALE DI FISICA NUCLEARE

Sezione di Genova

INFN/AE-05/04
May 19, 2005

COMPARISON OF GEANT4 ELECTROMAGNETIC PHYSICS MODELS AGAINST THE NIST REFERENCE DATA

Katsuya Amako[1], Susanna Guatelli[2], Vladimir N. Ivanchenko[3], Michel Maire[4], Barbara Mascialino[2], Koichi Murakami[1], Petteri Nieminen[5], Luciano Pandola[6], Sandra Parlati[6], Maria Grazia Pia[2], MichelaPiergentili2, Takashi Sasaki[1], Laszlo Urban[3]

[1)]KEK, Tsukuba, Ibaraki, Japan
[2)]INFN, Sezione di Genova, I–16146 Genova, Italy
[3)]CERN, CH 1122, Geneva, Switzerland
[4)]LAPP, Annecy, France
[5)]ESA, 2201 AZ Noordwijk ZH, The Netherlands
[6)]INFN Laboratori Nazionali del Gran Sasso, 67010 Assergi, L'Aquila, Italy
[7)]KFKI Research Institute for Particle and Nuclear Physics, H–1121 Budapest, Hungary

Abstract

The Geant4 Simulation Toolkit provides an ample set of physics models describing electromagnetic interactions of particles with matter. This paper presents the results of a series of comparisons for the evaluation of Geant4 electromagnetic processes with respect to NIST reference data. A statistical analysis was performed to estimate quantitatively the compatibility of Geant4 electromagnetic models with NIST data; the statistical analysis also highlighted the respective strengths of the different Geant4 models.

PACS:11.30.Er,13.20.Eb;13.20Jf;29.40.Gx;29.40.Vj

To be published on:
IEEE Transactions on Nuclear Science

Published by ***SIS–Pubblicazioni***
Laboratori Nazionali di Frascati

1 Introduction

Geant4 is an object oriented toolkit [1] for the simulation of the passage of particles through matter. It offers an ample set of complementary and alternative physics models for electromagnetic and hadronic interactions, based on theory, experimental data or parameterisations.

The validation of Geant4 physics models with respect to authoritative reference data is a critical issue, fundamental to establish the reliability of Geant4-based simulations. This paper is focused on the validation of Geant4 electromagnetic models, with the purpose to evaluate their accuracy and to document their respective strengths. It presents the results of comparisons of Geant4 electromagnetic processes of photons, electrons, protons and α particles with respect to reference data of the NIST (United States National Institute of Standards and Technologies) [2] -[3] and of the ICRU (International Commission on Radiation Units and Measurements) [4] -[5].

The simulation results were produced with Geant4 version 6.2. The Geant4 test process verifies that the accuracy of the physics models will not deteriorate in future versions of the toolkit with respect to the results presented in this paper.

2 Overview of Geant4 electromagnetic physics packages

The Geant4 Simulation Toolkit includes a number of packages to handle the electromagnetic interactions of electrons, muons, positrons, photons, hadrons and ions. Geant4 electromagnetic packages are specialised according to the particle type they manage, or the energy range of the processes they cover.

The physics processes modeled in Geant4 electromagnetic packages include: multiple scattering, ionisation, Bremsstrahlung, positron annihilation, photoelectric effect, Compton and Rayleigh scattering, pair production, synchrotron and transition radiation, Cherenkov effect, refraction, reflection, absorbtion, scintillation, fluorescence, and Auger electrons emission [1].

Alternative and complementary models are provided in the various packages for the same process. The Geant4 electromagnetic models studied in this paper are listed in Table 1.

2.1 Standard electromagnetic package

The Geant4 Standard electromagnetic package [8] provides a variety of models based on an analytical approach, to describe the interactions of electrons, positrons, photons, charged hadrons and ions in the energy range 1 keV - 10 PeV.

Table 1: Geant4 electromagnetic models in this comparison study.

Particle	Geant4 Models in Electromagnetic Packages
Photon	Geant4 Low Energy - EPDL Geant4 Low Energy - Penelope Geant4 Standard
Electron	Geant4 Low Energy - EEDL Geant4 Low Energy - Penelope Geant4 Standard
Proton	Geant4 Low Energy - ICRU 49 Geant4 Low Energy - Ziegler 1985 Geant4 Low Energy - Ziegler 2000 Geant4 Standard
α	Geant4 Low Energy - ICRU 49 Geant4 Low Energy - Ziegler 1977 Geant4 Standard

The models assume that the atomic electrons are quasi free; their binding energy is neglected except for the photoelectric effect; the atomic nucleus is assumed to be fixed and its recoil momentum is neglected.

2.2 Low Energy electromagnetic package

The Geant4 Low Energy electromagnetic package [9] -[10] extends the coverage of electromagnetic interactions in Geant4 below 1 keV, an energy range that is not covered by the Standard package. It handles the interactions of electrons, positrons, photons, charged hadrons and ions, offering different sets of models for each of the physics processes involved.

The interactions of electrons and photons are described by two sets of models. The set of models based on a parameterised approach exploits evaluated data libraries (EPDL97 [11], EEDL [12] and EADL [13]); these data sets are used to calculate cross sections and to sample the final state.

Another set of models for electrons, positrons and photons is based on an approach combining numerical databases and analytical models for the different interaction mechanisms [14] -[15]. These models were originally developed for the Penelope Monte Carlo FORTRAN code [16], and have been re-engineered into Geant4 with an object-oriented design.

Low energy processes are also available to handle the ionisation by hadrons and ions [17] -[18]. Different models, specialised for energy range, particle type and charge,

are provided. In the high energy domain ($>$ 2 MeV) the Bethe-Bloch formula is applied; below 1 keV the interactions are described by the free electron gas model. In the intermediate energy range parameterised models based on experimental data from the Ziegler [19] -[**?**] and ICRU [5] reviews are implemented; corrections due to the molecular structure of materials and the effect of the nuclear stopping power are also taken into account. The Barkas effect is described by means of a specialised model.

3 The comparison tests

The comparison study described in this paper addresses a set of physical quantities in the scope of the publicly available NIST reference databases. This collection of data represents an authoritative reference in the physics domain, also in the definition of protocols adopted in medical physics. The method used to generate the NIST data has been developed by a committee supported by the ICRU [4] -[5].

The comparison tests of Geant4 simulations against NIST reference data concern:

- the total photon attenuation coefficients,
- the cross sections of the individual processes of photons,
- the stopping power and the range of electrons, protons and α particles in the CSDA (Continuous Slowing Down Approximation).

The tests are performed on a selection of materials, covering the whole periodic element table: beryllium, germanium, aluminum, silicon, iron, cesium, silver, gold, lead, uranium.

The experimental set-up reproduced in the simulation is specific to each of the physics quantities under test, and corresponds to the conditions in which the reference data were obtained. In all the simulations the ionisation potentials of the selected materials were modified with respect to the default values in Geant4 [6], and were set as in the NIST [7].

The simulation results derived from each of the Geant4 electromagnetic physics models are compared to the NIST reference data with statistical methods. The goodness-of-fit test results provide an objective quantitative evaluation of the accuracy of each model.

4 Test of Geant4 photon processes

4.1 Reference data: the NIST-XCOM database

The NIST-XCOM database [2] provides photon scattering data and attenuation coefficients between 1 keV and 100 GeV for all the elements of the periodic table. It lists total

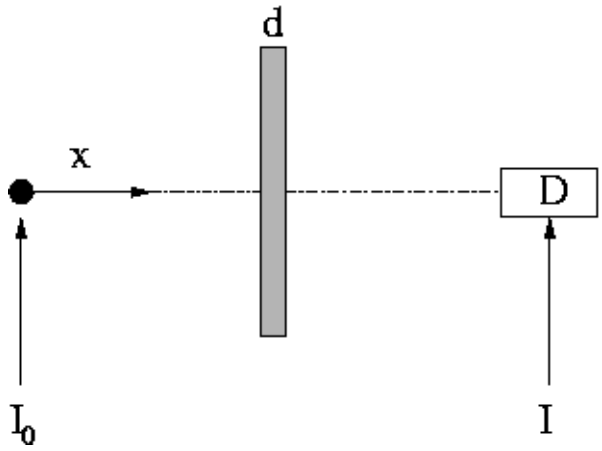

Figure 1: Experimental set-up adopted in the photon attenuation coefficients test: a monochromatic photon beam I_0 impinges on a slab of material. The primary photons emerging unperturbed from the slab are counted.

cross sections, attenuation coefficients and partial interaction coefficients for specific processes (Compton and Rayleigh scattering, photoelectric absorption, and pair production).

This database is based on [22] -[23] for incoherent and coherent scattering cross sections, on [24] for photoelectric absorption and on [25] for pair production. The authors state that the uncertainties in the values provided are rather difficult to estimate, depending on the energy range of the photons; they range from 1% to 5%, with the lowest and highest energy regions associated with larger uncertainties [26].

4.2 Geant4 simulation

Figure 1 shows the experimental set-up of the simulation, consisting of a monochromatic photon beam impinging on a slab of one of the selected materials. The thickness of the slab is optimised according to the energy of the incident beam, to avoid that all the photons are absorbed in the target or traverse the slab without interacting. The primary photons emerging unperturbed from the slab are counted. The energy range of incident photons varied between 1 keV and 100 GeV.

The Geant4 processes for photoelectric effect, Compton effect and pair production were activated for each of the packages under test. The process for Rayleigh effect was

activated for the Low Energy package; it is not available in the Geant4 Standard package.

For each of the simulation data sets 10.000 primary events were generated; the simulation uncertainties vary from point to point and are approximately 3%.

The photon mass attenuation coefficient $\frac{\mu}{\rho}$ is calculated as:

$$\frac{\mu}{\rho} = -\frac{1}{\rho d} ln\Big(\frac{N}{N_0}\Big) \tag{1}$$

where ρ represents the density of the target material, d is the thickness of the slab along the incident photon direction, N_0 is the number of incident photons, N is the number of photons traversing the target without interacting.

A partial interaction coefficient $(\frac{\mu}{\rho})_p$ can be calculated considering only a single interaction process (Rayleigh scattering, Compton scattering, pair production, photoelectric effect). This coefficient is related to the cross section of that process according to the equation:

$$\sigma_p = \frac{A}{N_{AV}} (\frac{\mu}{\rho})_p \tag{2}$$

where A represents the atomic mass of the target material and N_{AV} is Avogadro number.

Figures 2-6 show the results of Geant4 simulations for the three sets of electromagnetic models together with the NIST-XCOM reference data, as an example of the tests performed on various materials. They concern the photon attenuation coefficient in iron (Fig. 2), the photoelectric absorption in germanium (Fig. 3), Compton scattering in silver (Fig. 4), pair production in gold (Fig. 5), and Rayleigh scattering in beryllium (Fig. 6). For the clarity and readability of figures, the NIST reference is graphically represented with a continuous line interpolating the data, while the corresponding uncertainties are omitted in the plots. All the simulation results lie within $\pm 3\sigma$ with respect to the corresponding NIST data.

5 Test of Geant4 electron processes

5.1 Reference data: the NIST-ESTAR database

The NIST-ESTAR database [3] provides stopping powers and ranges of electrons as a function of energy between 10 keV and 1 GeV, derived from ICRU Report 37 [4].

Collision stopping powers are calculated from the theory of Bethe [27] -[28], with a density effect correction evaluated according to Sternheimer [29] -[30]. The uncertainties of the calculated collision stopping powers depend on the material and on the energy range, and are comprised between 1% and 10% [4]. Uncertainties increase at low energies.

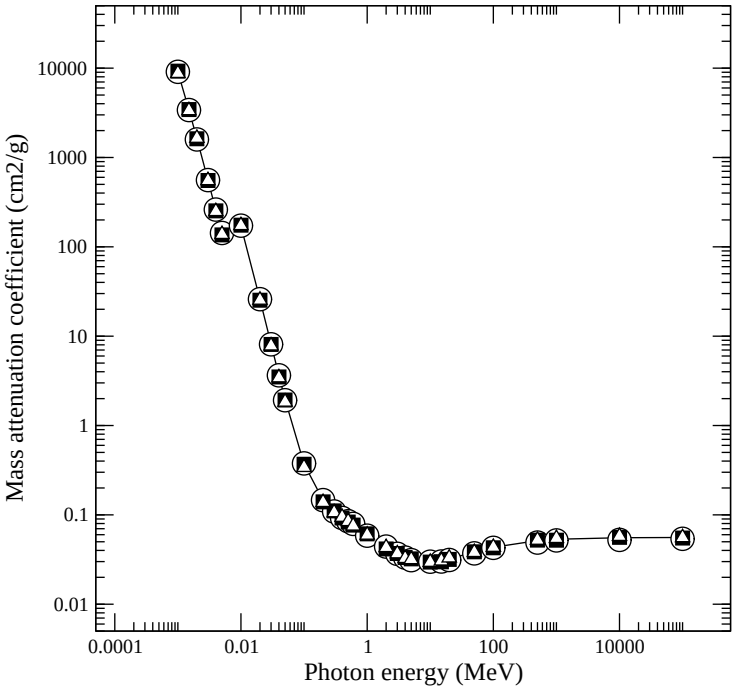

Figure 2: Mass attenuation coefficient in iron as a function of the photon incident energy for the three sets of Geant4 models under test (circles: Low Energy EPDL; squares: Low Energy Penelope; triangles: Standard); the continuous line interpolates NIST-XCOM reference data.

Radiative stopping powers are evaluated in NIST-ESTAR with a combination of theoretical Bremsstrahlung cross sections described by [31]. Analytical formulae, using a high energy approximation, are used above 50 MeV, and accurate numerical results of [32] below 2 MeV. Uncertainties range between 2% and 5%.

5.2 Geant4 simulation

The geometrical set-up of the simulation consists of a box of material, selected among those listed in Section III. Electrons are generated with random direction at the center of the box, with energy between 10 keV and 1 GeV and stop inside it.

The physics processes of ionisation and Bremsstrahlung are activated in the simulation for each of the Geant4 packages and models under test. To reproduce the conditions of the continuous slowing down approximation of the NIST-ESTAR database, multiple scattering and energy loss fluctuations were not activated in the simulation, and secondary particles were not generated. The maximum step allowed in tracking particles was set at approximately 1/10 of the expected range value, to ensure the accuracy of the calculation. In the continuous slowing down approximation the simulation is reduced to an analytical

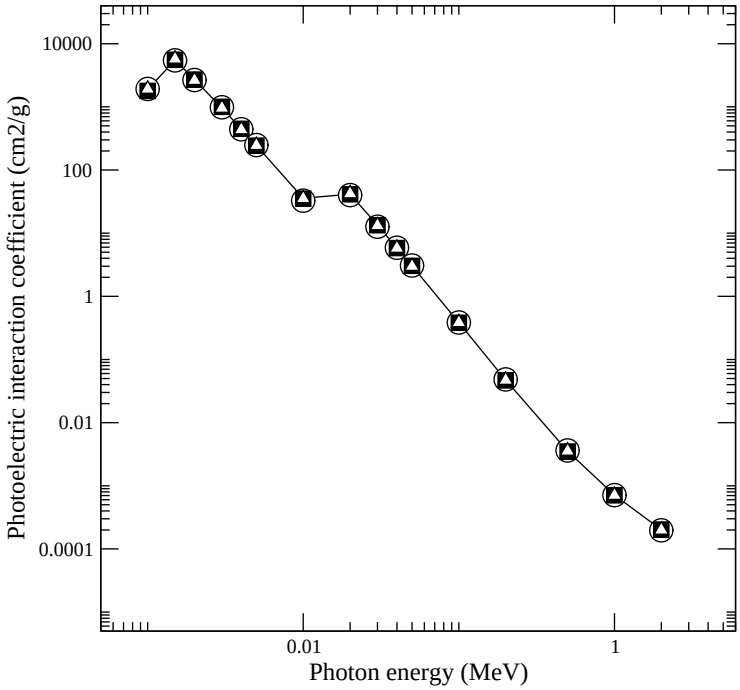

Figure 3: Photoelectric interaction coefficient in germanium as a function of the photon energy for the three sets of Geant4 models under test (circles: Low Energy EPDL; squares: Low Energy Penelope; triangles: Standard); the continuous line interpolates NIST-XCOM reference data. The interaction coefficient is related to photoelectric cross section as in equation (2).

calculation, since no fluctuations are generated; therefore the results are not subject to any statistical uncertainties.

The stopping power (SP) is calculated as:

$$SP = \frac{dE}{\rho\, dx} \tag{3}$$

where *dE* is the energy lost by the electron in a step of length *dx* in the material, and ρ is the density of the material.

The CSDA range is calculated as the distance between the point where the electron originates and the point where it stops, times the density of the material.

Figure 7 shows the range of electrons in uranium for the three sets of Geant4 models under test together with the NIST-ESTAR reference data, as an example of the results obtained for the various materials. All the simulation results lie within $\pm 3\sigma$ with respect to the corresponding NIST data.

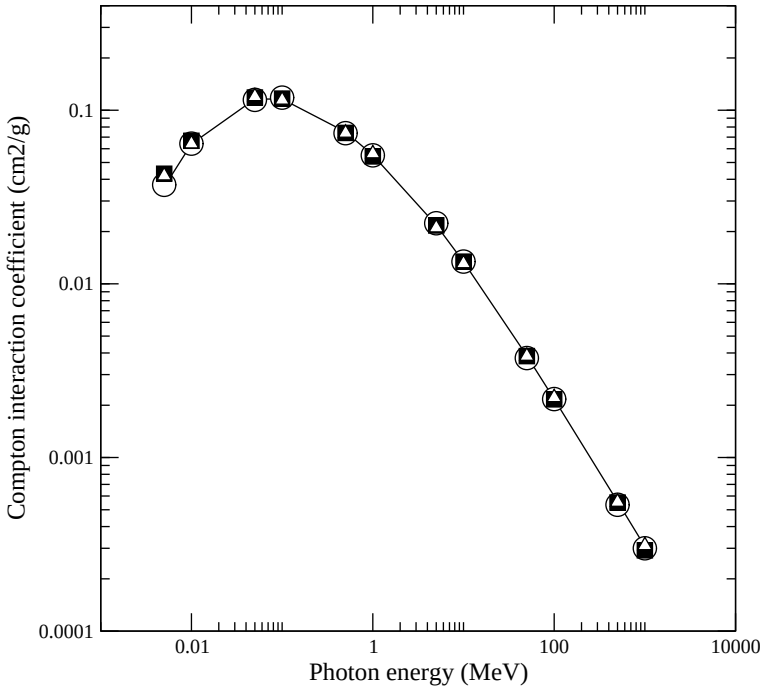

Figure 4: Compton interaction coefficient in silver as a function of the photon incident energy for the three sets of Geant4 models under test (circles: Low Energy EPDL; squares: Low Energy Penelope; triangles: Standard); the continuous line interpolates NIST-XCOM reference data. The interaction coefficient is related to Compton cross section as in equation (2).

6 Test of Geant4 proton and α processes

6.1 Reference data: the NIST-PSTAR and ASTAR databases

The NIST-PSTAR [19] and NIST-ASTAR [34] databases provide stopping powers and ranges of protons and α in the energy intervals 1 keV - 10 GeV and 1 keV - 1 GeV respectively, derived from ICRU Report 49 [5]. At high energies, collision stopping powers are evaluated using Bethe's stopping power formula [27]. At low energies, parameterisations based on experimental stopping power data are used [33]. The boundary between the high and low energy regions is approximately 0.5 MeV for protons, and 2 MeV for α particles.

The uncertainties of the collision stopping powers [5] are stated to be between 1% and 4% in the high energy region; in the low energy region they vary between 2% and 5% at 1 MeV, between 10% and 15% at 10 keV, and are at least 20% - 30% at 1 keV.

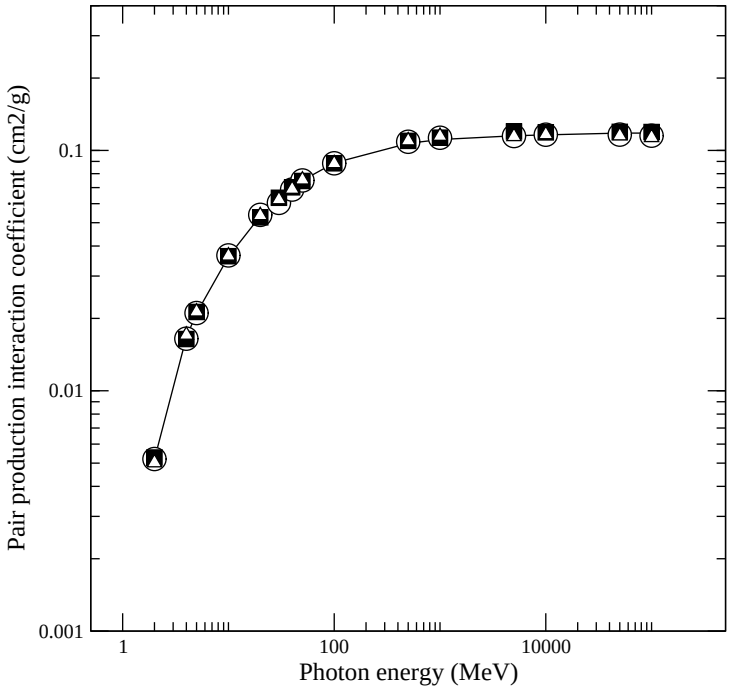

Figure 5: Pair production interaction coefficient in gold as a function of the photon incident energy for the three sets of Geant4 models (circles: Low Energy EPDL; squares: Low Energy Penelope; triangles: Standard); the continuous line interpolates NIST-XCOM reference data. The interaction coefficient is related to pair production cross section as in equation (2).

6.2 Geant4 simulation

The geometrical set-up of the simulation is the same as in the test for electron processes (Section V B.). Protons and α particles are generated with energies in the range 1 keV - 10 GeV and 1 keV - 1 GeV respectively.

The ionisation process was activated in the simulation for each of the Geant4 packages and models under test. The same conditions as described in Section V B. were set to reproduce the continuous slowing down approximation corresponding to the reference data. Particle ranges and stopping powers are calculated as in Section V B. In the continuous slowing down approximation the simulation is reduced to an analytical calculation, since no fluctuations are generated; therefore the results are not subject to any statistical uncertainties.

Figures 8 and 9 show the stopping power of protons in aluminum and the CSDA range of α particles in silicon for the sets of Geant4 models under test together with the NIST-PSTAR and NIST-ASTAR reference data respectively, as an example of the results obtained for the various materials. The $\pm 3\sigma$ interval around the NIST reference data is

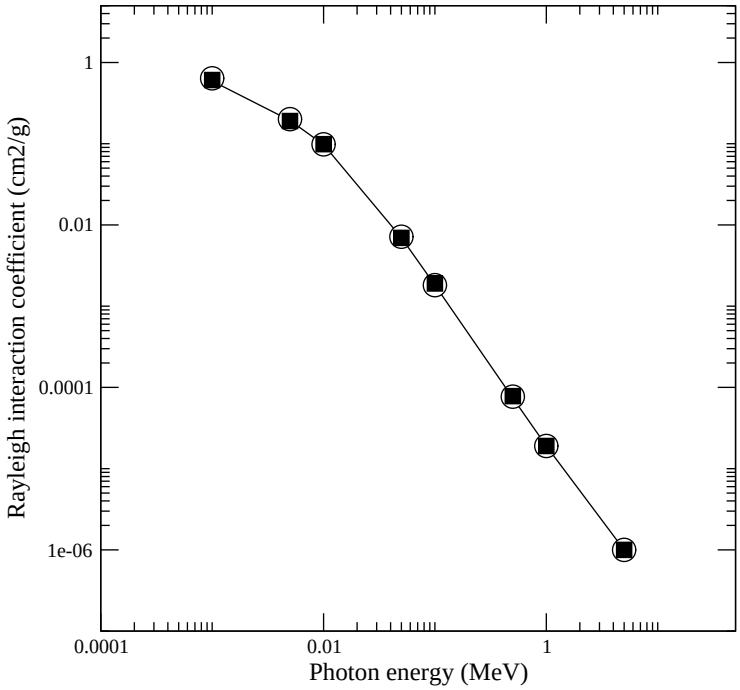

Figure 6: Rayleigh interaction coefficient in beryllium as a function of the photon incident energy for the two sets of Geant4 models under test (circles: Low Energy EPDL; squares: Low Energy Penelope); the continuous line interpolates NIST-XCOM reference data. The interaction coefficient is related to Rayleigh cross section as in equation (2).

identified by dashed lines in the figures.

7 Statistical analysis

Quantitative comparisons between NIST reference data and Geant4 simulations were performed by means of a Goodness-of-Fit Statistical Toolkit [35], specialised in the comparison of data distributions. A statistical comparison was executed for each of the Geant4 electromagnetic packages and models listed in Table I. For every physical quantity of interest and for every material considered, the aim of the comparison was to test whether the Geant4 simulation results agreed with the reference data over the whole energy range of the test.

From a statistical point of view, the two hypotheses under test were the following:

1. the null hypothesis stated the equivalence between reference data and Geant4 simulations for all energies $\mathrm{E_i}$:

$$\mathrm{H_0 : F_{Geant4}(E_i) = G_{NIST\ data}(E_i)},$$

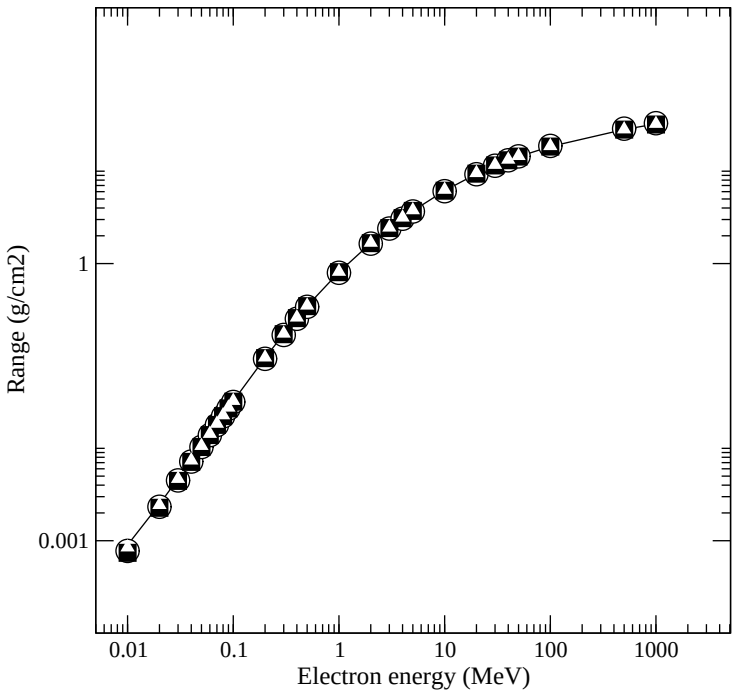

Figure 7: Electron CSDA range in uranium as a function of the electron incident energy for the three sets of Geant4 models under test together with the NIST-ESTAR reference data for the three sets of Geant4 models under test (circles: Low Energy EEDL; squares: Low Energy Penelope; triangles: Standard); the continuous line interpolates NIST-ESTAR reference data.

2. the alternative hypothesis stated that the two sets of data differed for at least one energy $\mathrm{E_i}$:

$$\mathrm{H_1 : F_{Geant4}(E_i) \neq G_{NIST\ data}(E_i)}.$$

The χ^2 test was selected among the ones available in the Goodness-of-Fit Statistical Toolkit, as this is the only algorithm including data uncertainties in the computation of the test statistics value.

The Goodness-of-Fit Statistical Toolkit returned the computed χ^2 value together with the number of degrees of freedom and the p-value of the comparison. The p-value represents the probability that the test statistics has a value at least as extreme as that observed, assuming that the null hypothesis $\mathrm{H_0}$ is true. A confidence level $\alpha = 0.05$ was set; p-values greater than α led to the acceptance of the null hypothesis $\mathrm{H_0}$.

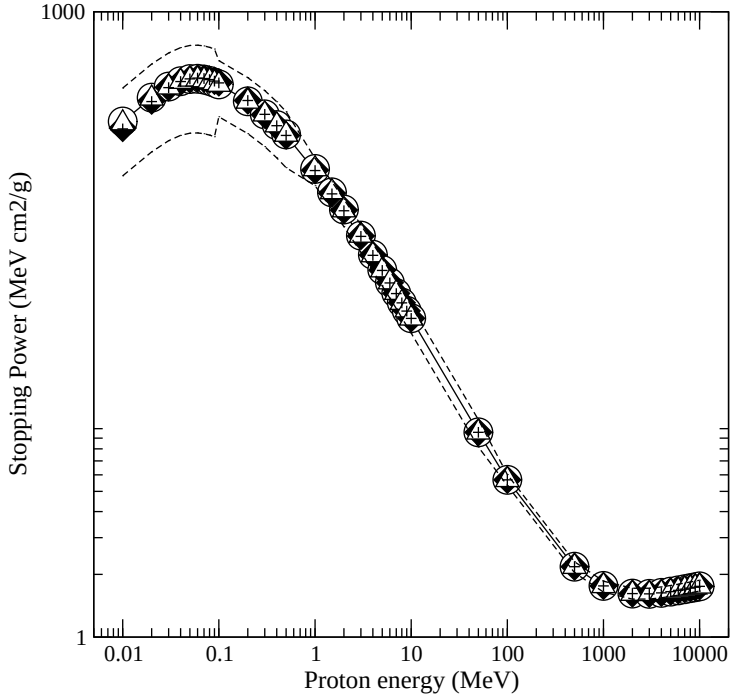

Figure 8: Proton stopping power in aluminum as a function of the proton incident energy for the different sets of Geant4 models under test (circles: Low Energy ICRU 49; diamonds: Low Energy Ziegler 1985; triangles: Standard; crosses: Low Energy Ziegler 2000); the continuous line interpolates NIST-PSTAR reference data. The dashed lines identify $\pm 3\sigma$ around the NIST reference data; the size of the data points is a visual artifact only; all the simulation results lie within $\pm 3\sigma$ with respect to the NIST reference.

8 Results and critical discussion

The statistical analysis of the data sets led to the acceptance of the null hypothesis H_0 for all the physics tests described in Sections IV, V and VI. Therefore, the goodness-of-fit tests demonstrate that Geant4 reproduces the reference data with high accuracy in the whole energy range, with any of its electromagnetic models.

8.1 Results of photon tests

The results of the χ^2 test on photon attenuation coefficients are shown in Figure 10 for the Geant4 Standard, Low Energy Parameterised and Low Energy Penelope models. The three Geant4 models reproduce total attenuation coefficients with high accuracy; the two Low Energy approaches exhibit the best agreement with reference data.

Table II reports the p-values of the χ^2 tests for each of the photon interaction cross sections studied. Concerning photoelectric absorption, all the three Geant4 models result

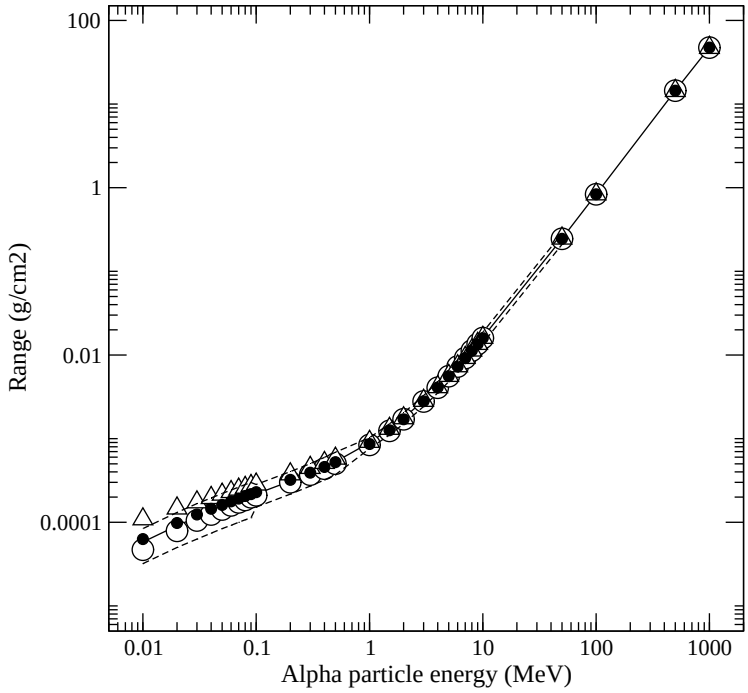

Figure 9: α particle CSDA range in silicon as a function of the α incident energy for the different sets of Geant4 models under test (empty circles: Low Energy ICRU 49; triangles: Standard; black circles: Low Energy Ziegler 1977); the continuous line interpolates NIST-ASTAR reference data. The dashed lines identify $\pm 3\sigma$ around the NIST reference data.

in agreement with the reference data; the two Geant4 Low Energy models exhibit the best agreement. Both Compton scattering and pair production are reproduced with high accuracy by the three Geant4 models. The Geant4 Low Energy Parameterised model exhibits the best overall agreement with reference data.

In the case of Rayleigh scattering, the Geant4 Low Energy models are in disagreement with the reference data for some materials. This disagreement is evident between 1 keV and 1 MeV photon energies. For what concerns the Geant4 Low Energy Parameterised model, the effect observed derives from an intrinsic inconsistency between Rayleigh cross section data in NIST-XCOM and the cross sections of EPDL97 [11] (Fig. 11), on which the Low Energy parameterised model is based. The coherent cross sections of EPDL97 are based on the combination of Thompson scattering, form factors and anomalous scattering factors; NIST-XCOM data are calculated as a combination of Thompson formula and of Hartree-Fock atomic form factors. Differences between EPDL97 and NIST-XCOM have already been highlighted in [36], which recommends the Livermore photon and electron data libraries [11] -[12] as the most up-to-date and accurate databases available for Monte Carlo modeling.

Table 2: Goodness-of-Fit results for each of the partial photon interactions studied in the test of photon processes.

	Geant4 model compared to XCOM data	Compton p-value	Photo-electric p-value	Pair production p-value	Rayleigh p-value
Be	Standard	0.85	0.63	1	- - -
	LowE-EPDL	1	1	1	0.99
	LowE-Penelope	1	1	1	1
Al	Standard	0.86	1	1	- - -
	LowE-EPDL	1	1	1	0.32
	LowE-Penelope	1	1	1	< 0.05
Si	Standard	0.77	1	1	- - -
	LowE-EPDL	0.09	1	1	0.77
	LowE-Penelope	1	1	1	< 0.05
Fe	Standard	0.99	1	1	- - -
	LowE-EPDL	1	1	1	1
	LowE-Penelope	0.75	1	1	< 0.05
Ge	Standard	0.96	1	1	- - -
	LowE-EPDL	1	1	1	< 0.05
	LowE-Penelope	0.07	1	1	0.39
Ag	Standard	0.92	1	1	- - -
	LowE-EPDL	1	1	1	0.36
	LowE-Penelope	0.79	1	1	0.08
Cs	Standard	0.78	0.27	0.99	- - -
	LowE-EPDL	1	0.94	1	< 0.05
	LowE-Penelope	0.97	1	0.99	< 0.05
Au	Standard	0.41	0.93	1	- - -
	LowE-EPDL	1	1	1	< 0.05
	LowE-Penelope	0.94	1	1	< 0.05
Pb	Standard	0.29	0.96	1	- - -
	LowE-EPDL	1	1	1	< 0.05
	LowE-Penelope	0.21	1	1	< 0.05
U	Standard	1	0.99	1	- - -
	LowE-EPDL	1	1	1	< 0.05
	LowE-Penelope	1	0.99	1	< 0.05

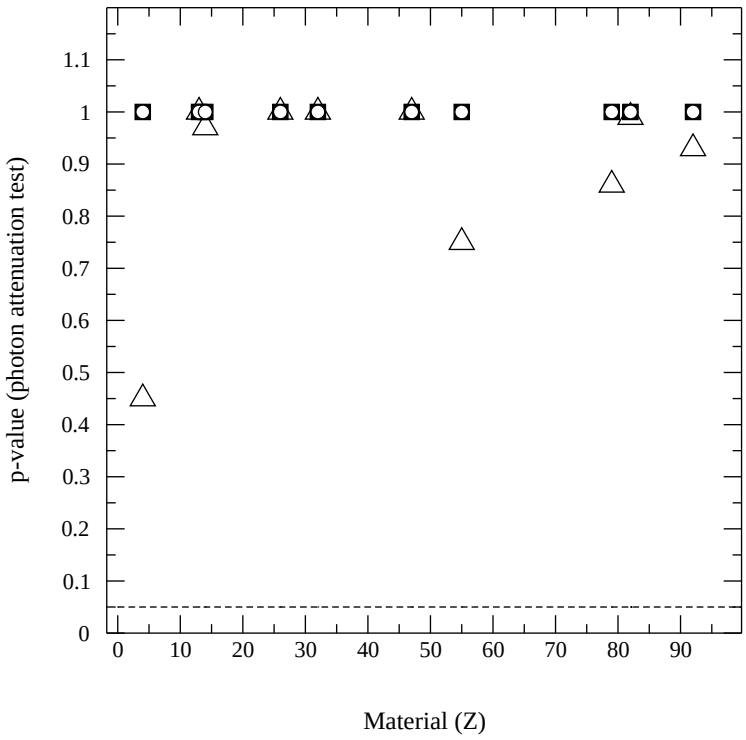

Figure 10: Results of the goodness-of-fit test concerning photon mass attenuation coefficient; the atomic number of the material is on the horizontal axis; the symbols represent Geant4 Standard (triangles), Low Energy EPDL (circles), and Low Energy Penelope (squares) models. The dashed line identifies the confidence level set for accepting the null hypothesis.

8.2 Results of electron tests

The results of the χ^2 test on electron stopping power and CSDA range are shown in Figures 12 and 13 respectively, for the Geant4 Standard, Low Energy Parameterised and Low Energy Penelope models.

The comparison test exhibited that all the Geant4 physics models are in excellent agreement with the NIST-ESTAR reference data; the test has not pointed out any particular difference among the three sets of models.

8.3 Results of proton and α tests

The results of the χ^2 test on proton stopping power and CSDA range and on α stopping power are shown in Figures 14-16 for the Geant4 Standard and Low Energy models.

The Geant4 Low Energy package contains a model directly based on the parameterisations of ICRU Report 49 [5], which are reported in the NIST database. For this model the comparison between Geant4 simulation results and reference data should be considered a software verification rather than a validation. The test showed some appar-

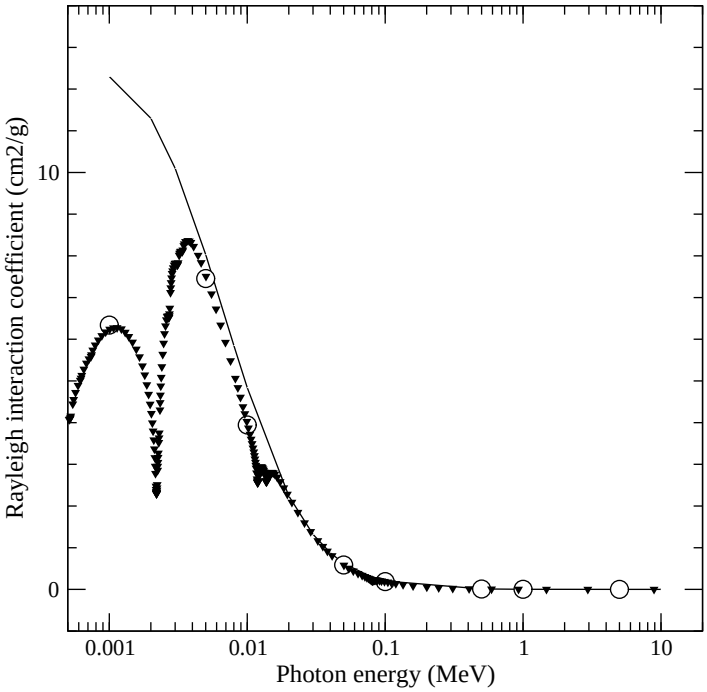

Figure 11: Comparison between Rayleigh interaction coefficient data from NIST-XCOM (continuous line) and EPDL97 (triangles) in the specific case of a gold slab. Note the major deviations between the two data sets. The results obtained with the Geant4 Low Energy package (circles) are in agreement with the EPDL97 data; this is meant to be a verification of the Geant4 simulation dedicated to this specific test. For more details see text.

ent discrepancies between the Low Energy models based on Ziegler parameterisations and the NIST reference. The Ziegler models represent an established reference in this physics domain, of relevance comparable to ICRU Report 49; in this case the comparison between the NIST reference and Geant4 models based on Ziegler parameterisations [19], [34] should be retained for its intrinsic interest, but it should not be considered as the validation of one set of parameterisations with respect to the other. In the higher energy region above a few MeV both the NIST reference data and all the Geant4 models follow the Bethe-Bloch formula; therefore, in this region the statistical comparison is a software verification and not a validation.

For some materials the Geant4 Standard electromagnetic package exhibits discrepancies with respect to the NIST reference data for α particles, especially in the lower energy region. The complex physics modeling [37] of ion interactions in the low energy range is addressed by the Geant4 Low Energy package; it represented indeed one of the main motivations for the development of this package.

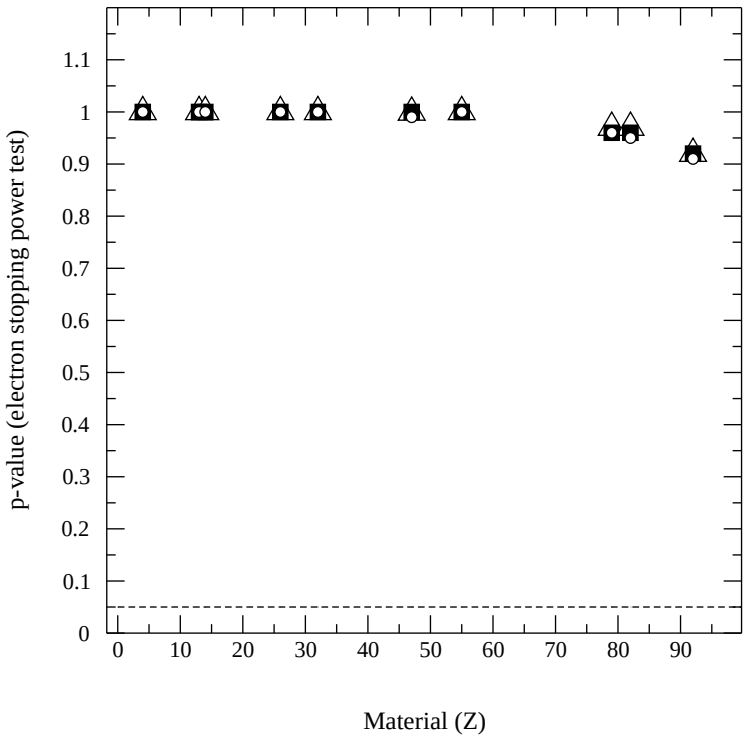

Figure 12: Results of the goodness-of-fit test concerning electron stopping power; the atomic number of the material is on the horizontal axis; the symbols represent Geant4 Standard (triangles), Low Energy EEDL (circles), and Low Energy Penelope (squares) models. The dashed line identifies the confidence level set for accepting the null hypothesis.

9 Conclusion

Systematic tests were performed to compare all the Geant4 electromagnetic models for electrons, photon, protons and α particles with respect to the NIST databases. The Geant4 models are found in good agreement with the reference data.

A quantitative statistical analysis allowed to document the respective strengths of the Geant4 models in detail, for each of the physics distributions considered in the NIST reference.

The flexible design of Geant4, based on object-oriented technology, allows the user to activate physics models in his/her simulation interchangeably from different packages; the quantitative documentation presented in this paper provides an objective guidance to select the Geant4 electromagnetic models most appropriate to any specific simulation application.

This work is part of a wider project for the systematic validation of Geant4 electromagnetic physics models, covering also other particle types, physics processes and energy ranges outside the scope of the NIST databases. Further quantitative comparisons

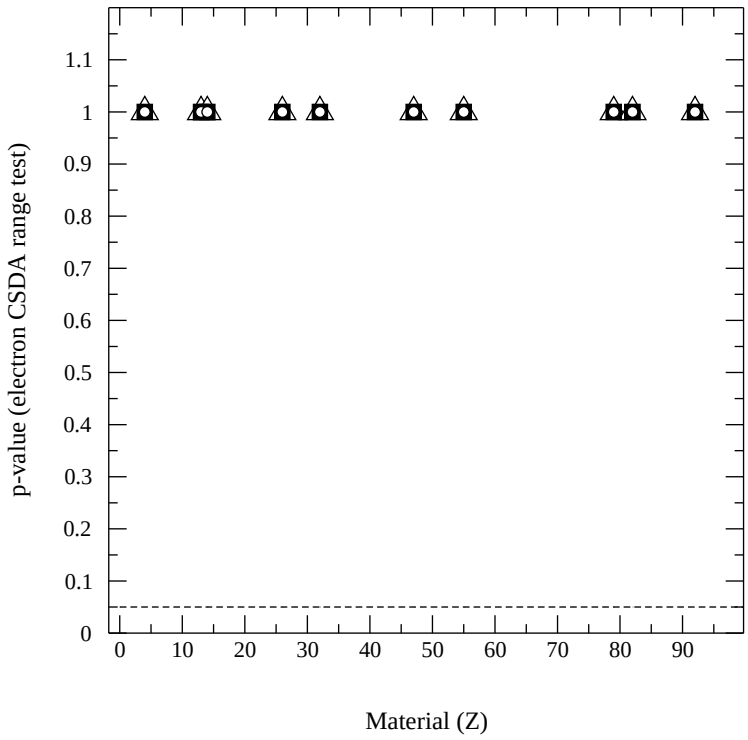

Figure 13: Results of the goodness-of-fit test concerning electron CSDA range; the atomic number of the material is on the horizontal axis; the symbols represent Geant4 Standard (triangles), Low Energy EEDL (circles), and Low Energy Penelope (squares) models. The dashed line identifies the confidence level set for accepting the null hypothesis.

of Geant4 electromagnetic processes with respect to other reference data will be the object of future papers.

10 Acknowledgements

The authors thank Andreas Pfeiffer for his support with data analysis software tools. The authors are grateful to Ian McLaren for proofreading this paper.

11 References

References

[1] S. Agostinelli, J. Allison, K. Amako, J. Apostolakis, H. Araujo, P. Arce, et al., “Geant4 - a simulation toolkit”, *Nucl. Instrum. Meth. A*, vol. 506, no. 3, pp. 250-303, 2003.

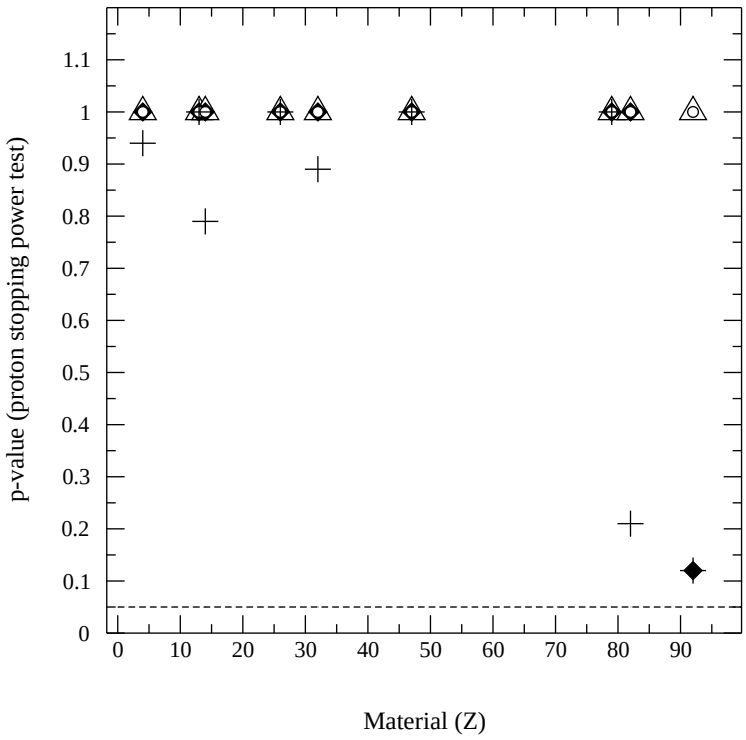

Figure 14: Results of the goodness-of-fit test concerning proton stopping power; the atomic number of the material is on the horizontal axis; the symbols represent Geant4 Standard (triangles), Low Energy ICRU 49 (circles), Low Energy Ziegler 1985 (diamonds), and Low Energy Ziegler 2000 (crosses) models. The dashed line identifies the confidence level set for accepting the null hypothesis.

[2] M. J. Berger, J. H. Hubbell, S. M. Seltzer, J. S. Coursey, and D. S. Zucker, "XCOM: photon cross section database (version 1.2)", National Institute of Standards and Technology, Gaithersburg MD, 1999.

[3] M. J. Berger, J. S. Coursey, and D. S. Zucker, "ESTAR, PSTAR, and ASTAR: computer programs for calculating stopping-power and range tables for electrons, protons, and helium ions (version 1.2.2)", National Institute of Standards and Technology, Gaithersburg, MD, 2000.

[4] ICRU International Commission on Radiation Units and Measurements, "ICRU Report 37, stopping powers for electrons and positrons", 1984.

[5] ICRU International Commission on Radiation Units and Measurements, "ICRU Report 49, stopping powers and ranges for protons and alpha particles", 1993.

[6] S. Ruben,*Handbook of the elements*. La Salle, IL: Open Court Publishing Co, 1995.

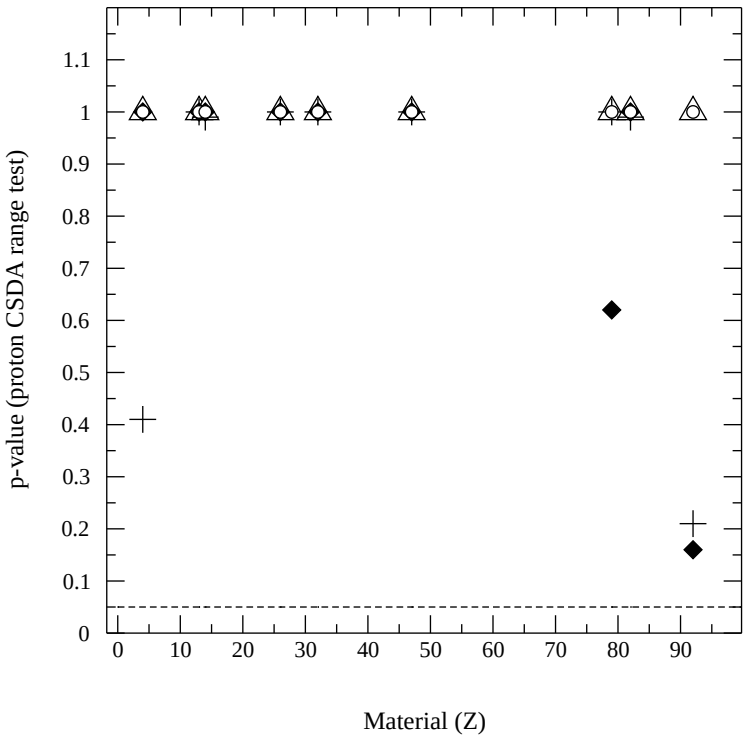

Figure 15: Results of the goodness-of-fit test concerning proton CSDA range; the atomic number of the material is on the horizontal axis; the symbols represent Geant4 Standard (triangles), Low Energy ICRU 49 (circle), Low Energy Ziegler 1985 (diamonds), and Low Energy Ziegler 2000 (crosses) models. The dashed line identifies the confidence level set for accepting the null hypothesis.

[7] W. C. Martin and W. L. Wiese "Atomic Spectroscopy", in *Atomic, Molecular, & Optical Physics Handbook*, G. W. F. Drake, Ed. Woodbury, NY: Amer. Inst. Phys., 1996, pp. 135-153.

[8] V. N. Ivanchenko, M. Maire, and L. Urban, "Geant4 Standard electromagnetic package for HEP applications", in *Conf. Rec. 2004 IEEE Nuclear Science Symposium*, N33-179.

[9] S. Chauvie, S. Guatelli, V. Ivanchenko, F. Longo, A. Mantero, B. Mascialino, et al., "Geant4 Low Energy electromagnetic physics", in *Conf. Rec. 2004 IEEE Nuclear Science Symposium*, N33-165.

[10] S. Chauvie, G. Depaola, V. Ivanchenko, F. Longo, P. Nieminen, and M. G. Pia, "Geant4 Low Energy electromagnetic physics", in *Proc. Computing in High Energy and Nuclear Physics*, Beijing, China, 2001, pp. 337-340.

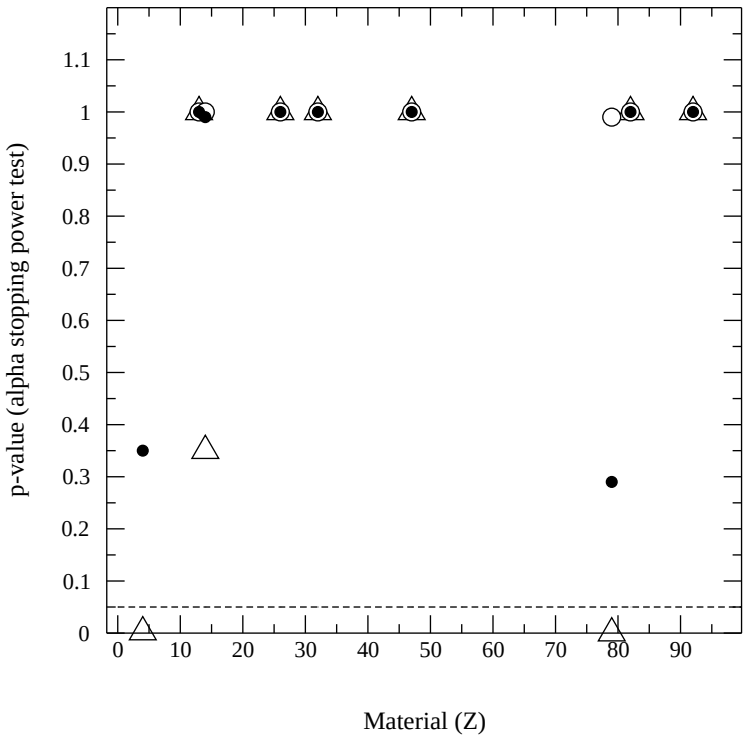

Figure 16: Results of the goodness-of-fit test concerning α stopping power; the atomic number of the material is on the horizontal axis; the symbols represent Geant4 Standard (triangles), Low Energy ICRU 49 (empty circles), and Low Energy Ziegler 1977 (black circles) models. The dashed line identifies the confidence level set for accepting the null hypothesis.

[11] D. Cullen, J. H. Hubbell, and L. Kissel, "EPDL97: the Evaluated Photon Data Library, '97 version", Lawrence Livermore National Laboratory, Rep. UCRL-50400, 1997, vol. 6, rev. 5.

[12] S. T. Perkins, D. E. Cullen, and S. M. Seltzer, "Tables and graphs of electron-interaction cross-sections from 10 eV to 100 GeV derived from the LLNL Evaluated Electron Data Library (EEDL), Z=1-100", Lawrence Livermore National Laboratory, Rep. UCRL-50400, 1997, vol. 31.

[13] S. T. Perkins, D. E. Cullen, M. H. Chen, J. H. Hubbell, J. Rathkopf, and J. Scofield, "Tables and graphs of atomic subshell and relaxation data derived from the LLNL Evaluated Atomic Data Library (EADL), Z=1-100", Lawrence Livermore National Laboratory, Rep. UCRL-50400, 1991, vol. 30.

[14] J. Sempau, E. Acosta, J. Baro, J. M. Fernández-Varea, and F. Salvat, "An algorithm for Monte Carlo simulation of coupled electron-photon transport", *Nucl. Instrum. Meth. B*, vol. 132, no. 3, pp. 377-390, 1997.

[15] J. Baro, J. Sempau, J. M. Fernández-Varea, and F. Salvat, “Penelope, an algorithm for Monte Carlo simulation of the penetration and energy loss of electrons and positrons in matter”, *Nucl. Instrum. Meth. B*, vol. 100, no. 1, pp. 31-46, 1995.

[16] J. Sempau, F. Salvat, J. M. Fernández-Varea, E. Costa, and J. Sempau, ”PENELOPE - a code system for Monte Carlo simulation of electron and photon transport”, in *Proc. Workshop Issy les Moulineaux*, France, 2001.

[17] S. Giani, V. N. Ivanchenko, G. Mancinelli, P. Nieminen, M. G. Pia, and L. Urban, ”Geant4 simulation of energy losses of slow hadrons”, INFN, Tech. Rep. INFN/AE-99/20, 1999.

[18] S. Giani, V. N. Ivanchenko, G. Mancinelli, P. Nieminen, M. G. Pia, and L. Urban, ”Geant4 simulation of energy losses of ions”, INFN, Tech. Rep. INFN/AE-99/21, 1999.

[19] H. H. Andersen and J. F. Ziegler, *The stopping and ranges of ions in matter*, vol.3, Ed. New York: Pergamon Press, 1977.

[20] J.F. Ziegler, J. P. Biersack, and U. Littmark, *The stopping and ranges of ions in solids*, vol.1, Ed. New York: Pergamon Press, 1985.

[21] J. F. Ziegler and J. P. Ziegler, “The stopping and range of ions in matter”, IBM-Research, Yorktown, NY, Tech. Rep., 2000.

[22] J. H. Hubbell, “Photon mass attenuation and energy absorption coefficients from 1 keV to 20 MeV”, *Int. J. Appl. Radiat. Isotopes*, vol. 33, no. 11, pp. 1269-1290, 1982.

[23] J. H. Hubbell, W. J. Veigele, E. A. Briggs, R. T. Brown, D. T. Cromer, and R. J. Howerton, “Atomic form factors, incoherent scattering functions, and photon scattering cross sections”, *J. Phys. Chem. Ref. Data*, vol. 4, no. 3, pp. 471-538, 1975.

[24] J. H. Hubbell and I .Overbo, “Relativistic atomic form factors and photon coherent scattering cross sections”, *J. Phys. Chem. Ref. Data*, vol. 8, no. 1, pp. 69-105, 1979.

[25] J. Leroux and T. P. Thinh, “Revised tables of X-ray mass attenuation coefficients”, Corporation Scientifique Classique, Quebec, 1977.

[26] D. E. Cullen, M. H. Chen, J. H. Hubbell, S. T. Perkins, E. F. Plechaty, J. A. Rathkopf, et al., “Tables and graphs of photon-interaction cross sections from 10 eV to 100 GeV derived from the LLNL Evaluated Photon Data Library (EPDL),

Part A: Z = 1 to 50; Part B: Z = 51 to 100", Lawrence Livermore National Laboratory, Livermore, Rep. UCRL-50400, 1989, vol. 6, rev. 4.

[27] H. A. Bethe, "Zur Theorie des Durchgangs schneller Korpuskularstrahlen durch Materie", *Ann. d. Physik*, vol. 5, pp. 325-400, 1930.

[28] H. A. Bethe, "Bremsformel fur Elektronen relativistischer Geschwindigket", *Zeitschrift fur Physik*, vol. 76, pp. 293-299, 1932.

[29] R. M. Sternheimer, "The density effect for the ionization loss in various materials", *Phys. Rev.*, vol. 88, no. 4, pp. 851-859, 1952.

[30] R. M. Sternheimer, S. M. Seltzer, and M. J. Berger, "Density effect for the ionization loss of charged particles", *Phys. Rev. B*, vol. 26, no. 11, pp. 6067-6076, 1982.

[31] S. M. Seltzer and M. J. Berger, "Bremsstrahlung spectra from electron interactions with screened atomic nuclei and orbital electrons", *Nucl. Instrum. Meth. B*, vol. 12 no. 1, pp. 95-134, 1985.

[32] R. H. Pratt, H. K. Tseng, C. M. Lee, L. Kissel, C. MacCallum, and M. Riley, "Bremsstrahlung energy spectra from electrons of kinetic energy 1 keV $< T_1 <$ 2000 keV incident on neutral atoms $2 <$ Z < 92", *Atomic data and nuclear data tables*, vol. 20, no. 2, pp. 175-209, 1977. Errata in vol. 26, no. 5, pp. 477-481, 1981.

[33] C. Varelas and J. Biersack, "Reflection of energetic particles from atomic or ionic chains in single crystals", *Nucl. Instrum. Meth.*, vol. 79, no. 2, pp. 213-218, 1970.

[34] J. F. Ziegler, "Helium: stopping powers and ranges in all elemental matter", in *The stopping and ranges of ions in matter*, vol. 4, Ed. New York: Pergamon Press, 1977.

[35] G. A. P. Cirrone, S. Donadio, S. Guatelli, A. Mantero, B. Mascialino, S. Parlati, et al., "A goodness-of-fit statistical toolkit", *IEEE Trans. Nucl. Sci.*, vol. 51, no. 5, pp. 2056-2063, Oct. 2004.

[36] H. Zaidi, "Comparative evaluation of photon cross section libraries for materials of interest in PET Monte Carlo simulation", *IEEE Trans. Nucl. Sci.*, vol. 47, no. 6, pp. 2722-2735, 2000.

[37] S. Giani, V. N. Ivanchenko, G. Mancinelli, P. Nieminen, M. G. Pia, and L. Urban, "Geant4 simulation of energy losses of ions", INFN Preprint, INFN/AE-99/21, 1999.